

Diverging Giant Magnetoresistance in the Limit of Infinitely Conducting Spacer

Soumen Mandal¹, R. C. Budhani^{1,*}, Jiaqing He², and Y. Zhu²

¹*Condensed Matter - Low Dimensional Systems laboratory, Department of Physics, Indian Institute of Technology Kanpur, Kanpur - 208016, India and*

²*Materials Science Department, Brookhaven National Laboratory, Upton, New York, 11973, USA*

Abstract

The relevance of pair-breaking by exchange and dipolar fields, and by injected spins in a low carrier density cuprate $Y_{1-x}Pr_xBa_2Cu_3O_7$ sandwiched between two ferromagnetic $La_{2/3}Sr_{1/3}MnO_3$ layers is examined. At low external field (H_{ext}), the system shows a giant magnetoresistance(MR), which diverges deep in the superconducting state. We establish a distinct dipolar contribution to MR near the switching field(H_c) of the magnetic layers. At $H_{ext} \gg H_c$, a large positive MR, resulting primarily from the motion of Josephson vortices and pair breaking by the in-plane field, is seen.

PACS numbers: 74.78.Fk, 74.72.Bk, 75.47.De, 72.25.Mk

Electron transport and magnetic ordering in ferromagnet (FM) - superconductor (SC) heterostructures display a plethora of novel phenomena[1, 2, 3, 4] which acquire increasing richness in systems where the nature of the FM and SC orders is exotic. Heterostructures of manganites and high temperature superconducting cuprates offer such systems[5]. The simplest structure which potentially can display some of these phenomena is a trilayer where a SC film is pressed between two ferromagnetic layers. Interest-

ingly, such a system in the normal state of the SC also constitutes the well-known spin valve in which two ferromagnetic layers sandwich a non-magnetic(NM) metallic spacer[6].

The giant negative magnetoresistance (MR) seen in FM-NM-FM trilayers and multilayers is related to asymmetric scattering of spin-up and spin-down electrons as they criss-cross the spacer while diffusing along the plane of the heterostructure[6]. This flow of spin polarized charges is expected to change profoundly when the spacer material becomes superconducting. Indeed,

*Electronic address: rcb@iitk.ac.in

a large MR has been seen by Pena et al[7] in $\text{La}_{0.7}\text{Ca}_{0.3}\text{MnO}_3$ - $\text{YBa}_2\text{Cu}_3\text{O}_7$ - $\text{La}_{0.7}\text{Ca}_{0.3}\text{MnO}_3$ trilayers in the narrow superconducting transition region which they attribute to spin accumulation in YBCO when the FM layers are coupled antiferromagnetically. These spins presumably cause depairing and hence a large positive MR in accordance with the spin imbalance theory of Takahashi, Imamura and Maekawa[8].

In this letter we examine the relevance of pair breaking by dipolar and exchange fields and injected spins in a low carrier density cuprate $\text{Y}_{1-x}\text{Pr}_x\text{Ba}_2\text{Cu}_3\text{O}_7$ (YPBCO) which has insulating c-axis resistivity and hence a poor spin transmittivity. We further address the issue of giant MR in $\text{La}_{2/3}\text{Sr}_{1/3}\text{MnO}_3$ - $\text{Y}_{1-x}\text{Pr}_x\text{Ba}_2\text{Cu}_3\text{O}_7$ - $\text{La}_{2/3}\text{Sr}_{1/3}\text{MnO}_3$ trilayers, in three distinctly illuminating ways which involve; i) current density dependence of MR over a broad range of temperature below T_c , ii) field dependence of MR when the magnetizations of $\text{La}_{2/3}\text{Sr}_{1/3}\text{MnO}_3$ (LSMO) layers \vec{M}_1 and \vec{M}_2 are parallel and fully saturated and, iii), dependence of MR on the angle between current and field below and above the critical temperature (T_c). These measurements permit disentanglement of the contributions of flux flow and pair breaking effects in YPBCO, and the intrinsic anisotropic MR of LSMO layers to GMR in FM-SC-FM trilayers, and establish a fun-

damental theorem which warrants diverging MR in the limit of infinitely conducting spacer.

Epitaxial trilayers of LSMO-YPBCO-LSMO were deposited on (001) SrTiO_3 . A multitarget pulsed laser deposition technique was used to deposit the single layer films and heterostructures as described in our earlier works [9]. The thickness of each LSMO layer (d_{LSMO}) was kept constant at 30nm where as the d_{YPBCO} was varied from 30 to 100nm. The interfacial atomic structure of the trilayers was examined with high resolution transmission electron microscopy (TEM) at Brookhaven National Laboratory.

The high quality of plane LSMO films and of the films integrated in FM-SC-FM heterostructures has been described in our previous reports[9]. We have also investigated superconductivity in $\text{Y}_{1-x}\text{Pr}_x\text{Ba}_2\text{Cu}_3\text{O}_7$ films as a function of Pr concentration[10]. As for single crystals[11], the T_c of the films[10] also decreases with Pr concentration, and for $x \geq 0.55$, the system has an insulating and antiferromagnetic (AF) ground state[12]. The reduction in T_c with x is presumed to be a consequence of lowering of the hole concentration and their mobility due to the out-of-plane disorder caused by Pr ions. Here we concentrate on $x = 0.4$ film because of its low carrier density and order parameter phase stiffness[10], both of which would enhance its

susceptibility to pair-breaking by spin polarized carriers injected from the LSMO.

Figure 1 shows the resistivity of a trilayer where the onset of hole localization in YPBCO before superconductivity sets in is indicated by the rise in resistivity near $\simeq 30$ K. The inset of Fig.1 shows a typical current (I) - voltage (V) characteristic of the structure at 15K. The figure also shows a cross-sectional TEM micrograph of the heterostructure. A sharp interface between LSMO and YPBCO is seen in this atomic resolution image. While the manganite layers are free of growth defects, we do see distinct stacking faults in the YPBCO, which can be related to disorder due to difference in ionic radii of Y^{3+} and Pr^{3+} .

Figure 2 (Panel a) shows the magnetic field (\vec{H}) dependence of magnetization (\vec{M}) at 10 K with \vec{H} in the plane of the heterostructure and parallel to the easy axis [110] of LSMO. Starting from a fully saturated magnetic state at $H \simeq 180$ Oe, the M reaches a plateau over a field range of -90 to -130 Oe on field reversal. This is indicative of AF alignment of the \vec{M} vectors of the top and bottom LSMO films. We have demonstrated earlier that the poor c-axis conductivity of YBCO actually quenched the oscillatory part of the interlayer exchange interaction and only an exponentially decaying AF-exchange remains in the LSMO-YBCO-LSMO system[9]. The full cancelation of the

moment ($M \simeq 0$) seen in the plateau also suggests that the two layers have equal saturation magnetization (M_s). In the remaining three Panels of Fig. 2 we show the in-plane resistance of the trilayer as a function of \vec{H} coplanar with the measuring current(I). Two values of the angle (θ) between the I and H have been chosen; in one case $\theta = 0^\circ$ (Fig. 2b) and for the other two panels (c & d), $\theta = 90^\circ$ but the magnitude of I is different. While these measurements have been performed at several currents, only a few representative field scans of MR are shown in Fig. 2. The MR for both $\theta = 90^\circ$ and $\theta = 0^\circ$ configurations has two distinct regimes of behavior. Starting from a fully magnetized state at 500 Oe and $\theta = 90^\circ$, the MR first drops to a minimum as the field is brought to zero following a dependence of the type $\sim \alpha H + \beta H^2$, where $\alpha = -6.8 \times 10^{-6}$ and $\beta = 7.7 \times 10^{-8}$ for $I = 0.8$ mA and $\theta = 90^\circ$. The MR shows a step-like jump at the reversed field of ~ 40 Oe where the magnetization switch to AF configuration and remains high till \vec{M}_1 and \vec{M}_2 become parallel again. One reversing the field towards positive cycle, a mirror image of the curve is seen in the positive field quadrant. A remarkable feature of the MR is its dependence on current I. The peak MR at 500 Oe drops from $\sim 80\%$ to 17% on increasing the current by a factor of two. The height of the MR curves

remains nearly the same when the magnetic field is rotated from $\theta = 90$ to $\theta = 0$ with some differences in its shape. The pertinent factors which affect the MR of such structures are; i) the MR in the normal state of YPBCO, ii) the explicit role of superconductivity which is suppressed by the dipolar and exchange fields of the FM layers, and by the spin polarized electrons injected from the FM layers, and iii), a parasitic non-zero tilt of the sample away from parallel configuration which will result in a high concentration of vortices in the superconducting spacer even at low fields. These factors are addressed with the help of Fig. 3 where we have plotted $M(H)$ loop at 40 K (normal state). The AF alignment of \vec{M}_1 and \vec{M}_2 in the vicinity of zero-field persists in the normal state as well. Figure 3 also shows the field-dependence of MR for $\theta = 90^\circ$ at a few temperatures as the sample is taken from superconducting to normal state. A striking drop in MR on approaching the normal state is evident in addition to a noticeable change in its field dependence. At 40 K, it drops monotonically on reducing the field from full saturation till the reverse switching field is reached where it shows a small but discernible step-like increase followed by an unremarkable field dependence in the negative field side. For $I \parallel H$ ($\theta = 0^\circ$) the $R(H)$ curve (not shown) reflects the anisotropic magnetoresistance (AMR) of

LSMO films.

It becomes clear from Fig. 2 and 3 that the H-dependence of MR in these FM-SC-FM trilayers can be divided into two regimes, one covering the range $-150\text{Oe} < H < 150\text{Oe}$ where the reorientation of \vec{M}_1 and \vec{M}_2 is the deciding factor, and at the higher fields where $\vec{M}_1 \parallel \vec{M}_2$ and it goes as $\sim \alpha H + \beta H^2$. While the MR in these regimes is intimately linked with superconductivity of YPBCO, its mechanism is different. First let us concentrate on the low-field regime where we define the MR as $(R_{\uparrow\downarrow} - R_{\uparrow\uparrow}) / R_{\uparrow\downarrow}$ where $R_{\uparrow\uparrow}$ and $R_{\uparrow\downarrow}$ are the resistances of the trilayer when \vec{M}_1 and \vec{M}_2 are parallel and antiparallel respectively. The variation of MR with $R_{\uparrow\downarrow}$ at a fixed T(15K) with variable I, and at several Ts across the transition at constant I is shown in Fig. 4. A remarkable universality of the dependence of MR emerges on the ground state resistance of the structure. The magnetoresistance starts with a negligibly small value at $T > T_c$ but then diverges on entering the superconducting state. While an enhancement in MR has been seen with cleaner spacers[6], the regime of diverging MR is only accessible with a superconducting spacer. Unlike the case of free-electron metal spacers, where the strength of MR is attenuated by spin flip scattering in the interior of the spacer and at spacer - ferromagnet interfaces[6], the physics of transport of spin polarized carri-

ers in FM-SC-FM structures is much more challenging. Here we identify various factors which can contribute to MR and then single out the ones, which, perhaps are truly responsible for the behavior seen in Fig. 4. In the inset of Fig. 4 we sketch a typical MR vs H curve at $T < T_c$ and mark on it some critical points where the orientation of \vec{M}_1 and \vec{M}_2 and the effective magnetic field seen by the SC layer change significantly. For the AF configuration (point C) the dipolar field of LSMO in the spacer cancels out but for the FM alignment (point B) it adds up. Thus, strictly from the angle of pairbreaking by the dipolar field, the SC layer should have a lower resistance in the AF configuration. Moreover, a much stronger effect of the exchange field of FM layers on superconductivity when \vec{M}_1 and \vec{M}_2 are parallel should make the AF state less resistive as shown originally by deGennes[1]. Both these effects are inconsistent with the observation of a higher resistance in the AF state. However, before we rule out the effect of the dipolar field altogether, a careful examination of the situation in the vicinity of $H_{ext} = 0$ shows that at the negative coercive field H_c , just before \vec{M}_1 and \vec{M}_2 become antiparallel, the internal field in SC $B_{\uparrow\uparrow} = -\mu_o H_{ext} - \mu_o(m_1^d + m_2^d)$, where m_1^d and m_2^d are the dipolar contribution to magnetization in the superconductor. This is what preferably result in increase in resis-

tance from point B to C in the inset. However, just beyond $H > H_c$ in the AF state, the internal field ($B_{\uparrow\downarrow}$) is only $\mu_o H_{ext}$ (assuming $m_1^d \sim m_2^d$). While this sudden reduction in B_{int} at H_c could be responsible for the plateau seen in $R(H)$ in the AF state, the higher resistance in the AF state still remains a puzzle. Although one could attribute it to piling up of spin polarized quasiparticles in SC spacer, such interpretation would require a deeper understanding of c-axis transport in these structures where the CuO_2 planes are parallel to the magnetic layers. The observation of this effect in a low carrier density cuprate of the present study is much more intriguing because its c-axis resistivity is insulator-like in the normal state[12].

We now discuss the large positive MR in the FM configuration of \vec{M}_1 and \vec{M}_2 . The H-dependence of MR in this regime derives contributions from pair breaking effects of spin polarized electrons injected from LSMO and of the net field seen by the YPBCO layer. Moreover, a parasitic normal component of the field due to misalignment will introduce vortices and a large dissipation due to flux flow. We have estimated the contribution of sample tilt by measuring its resistance in two configurations P and Q as shown in Fig. 5(a&b). We assume that the sample platform, instead of being on the x-y plane, has a small tilt δ away from the y-axis. In P, the

sample is mounted in such a manner that the stripe of film is nominally along \hat{y} . Fig. 5(b) shows the 90° geometry such that the stripe is now along the \hat{x} . We rotate \vec{H} in the xy-plane and measure R as a function of the angle θ between \hat{y} and the field direction. We expect three distinct contributions to $R(\theta)$ coming from; i) Vortex dissipation due to normal component of the field $[(\Delta R)_{v\perp}]$, ii) Lorentz force on Josephson vortices in the plane of the film $(\Delta R)_{v\parallel}$, and iii), the AMR of LSMO layers $(\Delta R)_{AMR}$ which peaks when I is perpendicular to the in-plane field[13]. While all these contributions to R are periodic in θ with a periodicity of π , in configuration P $(\Delta R)_{v\perp}$ will peak at $\theta = 0$ and π where as the peak in $(\Delta R)_{v\parallel}$ and $(\Delta R)_{AMR}$ will appear at $\theta = \pi/2$ and $3\pi/2$. Since the resistivity of the sample in configuration ‘P’ peaks at $\pi/2$ and $3\pi/2$ (see Fig. 5(c)), it is evident that $(\Delta R)_{v\perp} < ((\Delta R)_{v\parallel} + (\Delta R)_{AMR})$. For configuration Q, on the other hand, $(\Delta R)_{v\perp}$, $(\Delta R)_{v\parallel}$ and $(\Delta R)_{AMR}$ are all in phase with peak value appearing at $\theta = 0$ and π as seen

in Fig. 5(c). Clearly, the difference of the peak height at $\theta = 0$ of Q and $\theta = \pi/2$ of P gives us the flux flow resistance due to motion of vortices nucleated by a non-zero tilt. Its contribution to resistance is $\sim 10\%$ at 15 K and 3kOe nominally parallel field. Of course its strength will also vary with current. It is clear that a much larger contribution to +ve MR comes from the in-plane field and its attendant effects.

In conclusion, we have examined the role of pair breaking interactions such as the dipolar field, exchange field and spin polarized quasiparticles, and of vortices in setting the large magnetoresistance of a FM-SC-FM heterostructure at $T < T_c$ of the SC layer. At low fields, we see a direct correlation between the MR and the resistance of the ground state where the FM layer are coupled antiferromagnetically.

This research has been supported by a grant from the Board of Research in Nuclear Sciences, Govt. of India.

[1] P. G. de Gennes, Phys. Lett. **23**, 10 (1966); G. Deutscher and F. Meunier, Phys. Rev. Lett. **22**, 395 (1969); J. J. Hauser, Phys. Rev. Lett. **23**, 374 (1969)
[2] F. S. Bergeret, A. F. Volkov and K. B. Efetov, Rev. Mod. Phys. **77**, 1321 (2005);

I. F. Lyuksyutov and V. L. Pokrovski, Advances in Physics **54**, 67 (2005); A. I. Buzdin, Rev. Mod. Phys. **77**, 935 (2005)
[3] J. Y. Gu, C.-Y. You, J. S. Jiang, J. Pearson, Ya. B. Bazaliy and S. D. Bader, Phys. Rev. Lett. **89**, 267001 (2002); R. S. Keizer,

- S. T. B. Goennenwein, T. M. Klapwijk, G. Miao, G. Xiao and A. Gupta, *Nature* **439**, 825 (2006); John Q. Xiao and C. L. Chien, *Phys. Rev. Lett.* **76**, 1727 (1996); E. A. Demler, G. B. Arnold and M. R. Beasley, *Phys. Rev. B* **55**, 15174 (1997)
- [4] V. Peña, T. Gredig, J. Santamaria and Ivan. K. Schuller, *Phys. Rev. Lett.* **97**, 177005 (2006); Zhaorong Yang, Martin Lange, Alexander Volodin, Ritta Szymczak and Victor V. Moshchalkov, *Nature Materials* **3**, 793 (2004); David J. Morgan and J. B. Ketterson, *Phys. Rev. Lett.* **80**, 3614 (1998)
- [5] C. A. R. Sá de Melo, *Physica C* **387**, 17 (2003); J. Chakhalian, J. W. Freeland, G. Srajer, J. Stremper, G. Khaliullin, J. C. Cezar, T. Charlton, R. Dalgliesh, C. Bernhard, G. Cristiani, H.-U. Habermeier and B. Keimer, *Nature Physics* **2**, 244 (2006); A. M. Goldman, V. Vas'ko, P. Kraus, K. Nikolaev and V. A. Larkin, *J. Mag. Mag. Mat.* **200**, 69 (1999)
- [6] K. B. Hathaway, *Ultrathin Magnetic Structures II*, edited by B. Heinrich and J. A. C. Bland (Springer-Verlag, Germany, 1994) p. 45-194
- [7] C. Visani, V. Peña, J. Garcia-Barriocanal, D. Arias, Z. Sefrioui, C. Leon, J. Santamaria, N. M. Nemes, M. Garcia-Hernandez, J. L. Martinez, S. G. E. te Velthuis and A. Hoffmann, *Phys. Rev. B* **75**, 054501 (2007); V. Peña, Z. Sefrioui, D. Arias, C. Leon, J. Santamaria, J. L. Martinez, S. G. E. te Velthuis and A. Hoffmann, *Phys. Rev. Lett.* **94**, 057002 (2005)
- [8] S. Takahashi, H. Imamura and S. Maekawa, *Phys. Rev. Lett.* **82**, 3911 (1999); S. Takahashi, H. Imamura and S. Maekawa, *J. Appl. Phys.* **87**, 5227 (2000)
- [9] K. Senapati and R. C. Budhani, *Phys. Rev. B* **71**, 224507 (2005); K. Senapati and R. C. Budhani, *Phys. Rev. B* **70**, 174506 (2004)
- [10] Pengcheng Li, Soumen Mandal, R. C. Budhani and R. L. Greene, *Phys. Rev. B* **75**, 184509 (2007)
- [11] V. Sandu, E. Cimpoiasu, T. Katuwal, Shi Li, M. B. Maple and C. C. Almasan, *Phys. Rev. Lett.* **93**, 177005 (2004)
- [12] R. F. Tournier, D. Isfort, D. Bourgault, X. Chaud, D. Buzon, E. Floch, L. Porcar and P. Tixado, *Physica C* **386**, 467 (2003); Ratan Lal, Ajay, R. L. Hota and S. K. Joshi, *Phys. Rev. B* **57**, 6126 (1998)
- [13] L. M. Berndt, Vincent Balbarin and Y. Suzuki, *Appl. Phys. Lett.* **77**, 2903 (2000)

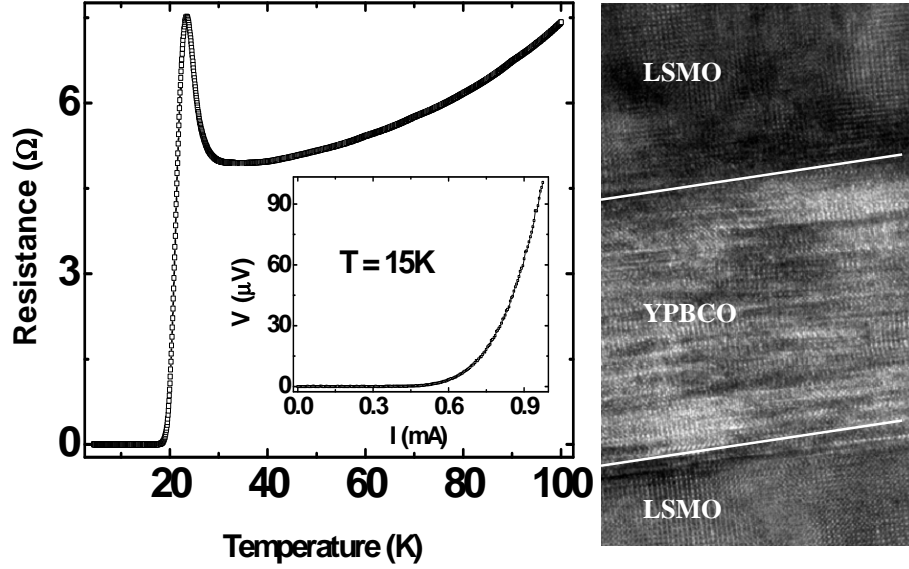


FIG. 1: R vs T curve for a LSMO - YPBCO - LSMO trilayer with 100nm YPBCO sandwiched between 30nm each of LSMO layers is shown in the left panel. The onset of hole localization in YPBCO before the superconductivity sets in is evident from the rise in resistivity near $\sim 30\text{K}$. The inset of left panel shows a typical I vs V characteristic of the trilayers at 15K. The right panel shows a high resolution cross sectional TEM of the trilayer with $d_{YPBCO} = 200\text{\AA}$.

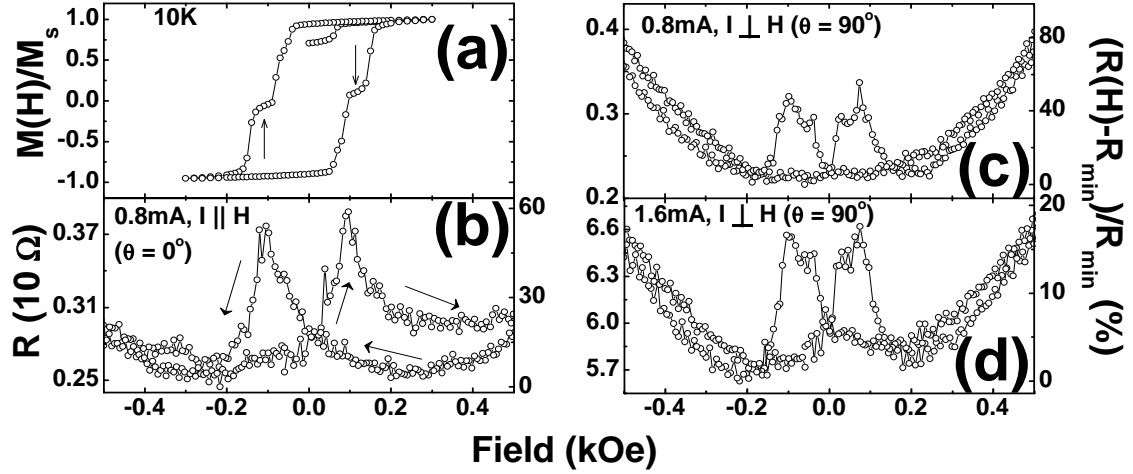


FIG. 2: Panel(a) shows M vs H loop of the trilayer taken at 10K. The two symmetric small plateaus(indicated by arrows), with zero magnetization show antiferromagnetic coupling between the two FM layers. Panel (b) to (d) show MR measured at 15K. The left hand side of y-axis shows resistance in units of 10Ω and the right hand y-axis shows the $(R(H) - R_{min})/R_{min}$ in %. In Panel (b) the current was parallel to field where as for the remaining two Panels, the in-plane field was orthogonal to the current ($\theta = 90^\circ$) which takes two values; 0.8 and 1.6 mA for (c) and (d) respectively.

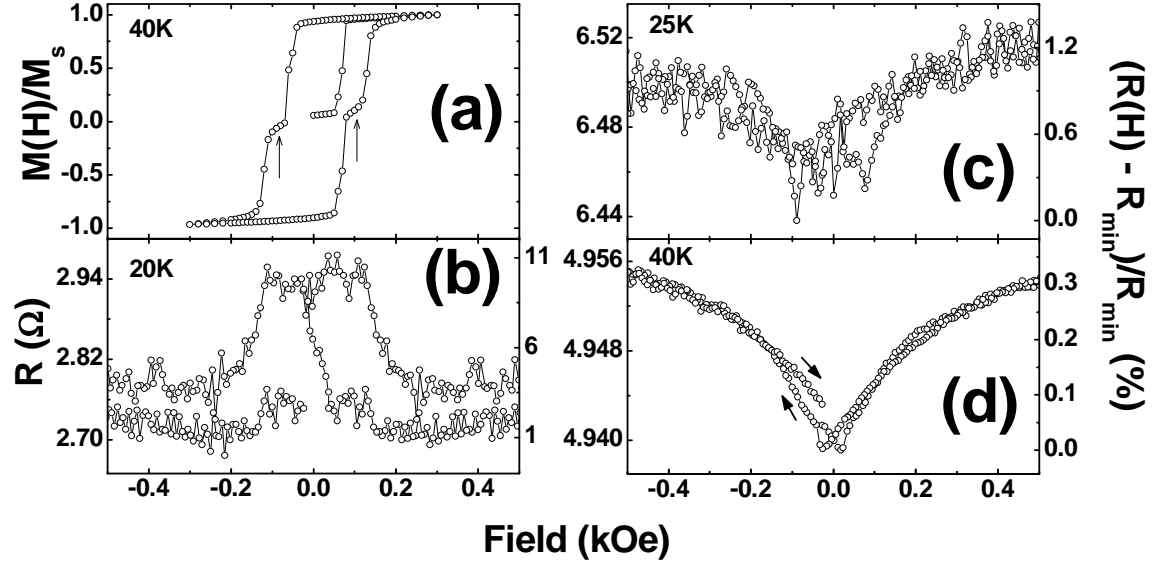


FIG. 3: (a) M vs. H loop for the trilayer taken at 40K. Two symmetric small plateaus (indicated by arrows) with zero magnetization show antiferromagnetic coupling between the two FM layers. Panels (b), (c) & (d) show field dependence of magnetoresistance in $\theta = \pi/2$ ($\vec{I} \perp \vec{H}$) configuration at 20, 25 and 40K respectively. The left hand side of y-axis shows resistance (Ω) and the right hand y-axis shows the $(R(H) - R_{min})/R_{min}$ in %.

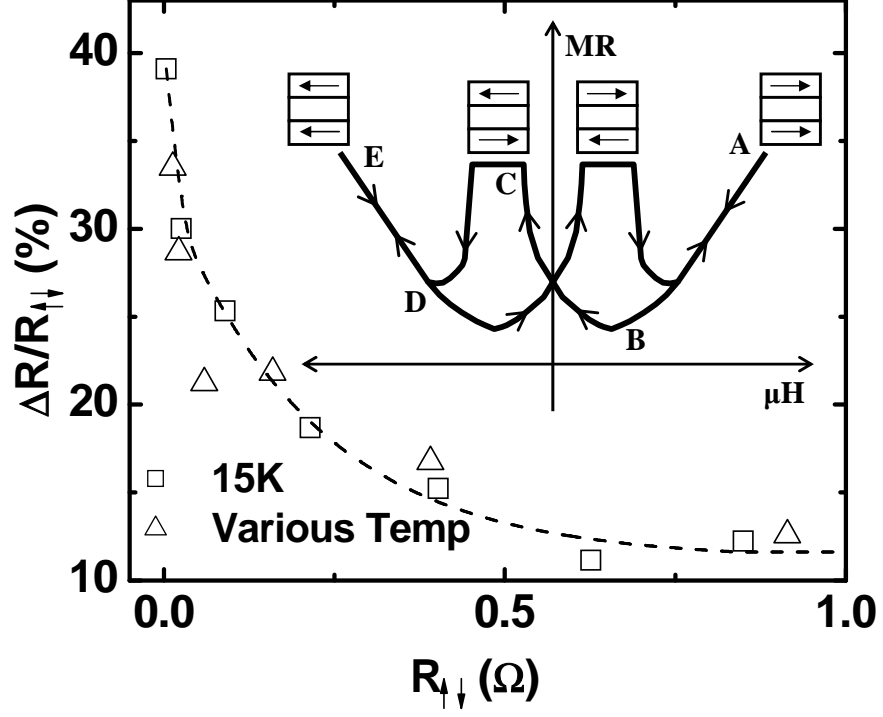


FIG. 4: Dependence of MR on $R_{\uparrow\downarrow}$. This figure contains MR data collected at 15K with variable current and at several temperatures across the transition at constant current. A remarkable universality of the dependence of MR emerges on the ground state resistance of the structure. The inset shows a typical sketch of MR vs H curve in the superconducting state and identify some critical points where \vec{M}_1 & \vec{M}_2 change their orientation (More details in text).

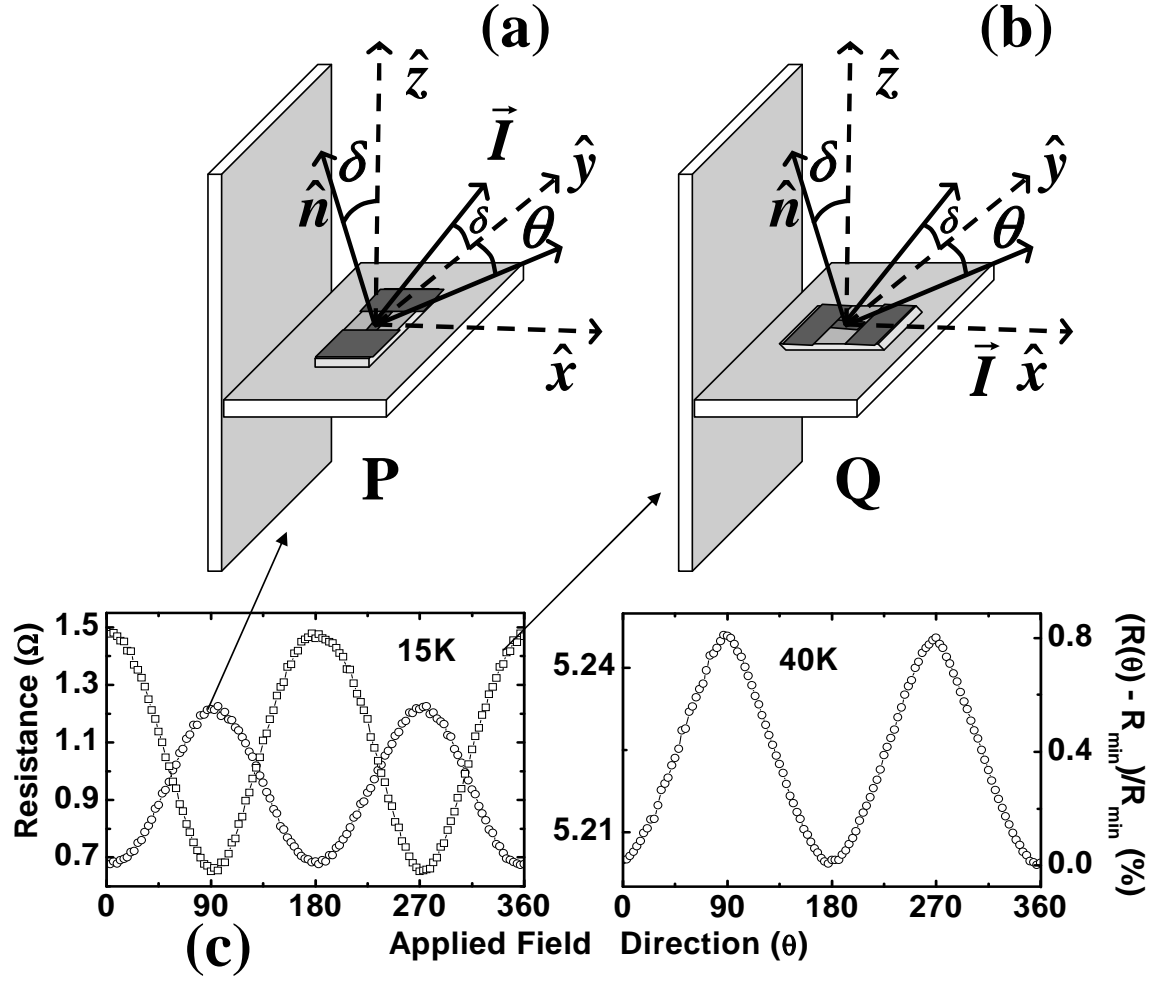


FIG. 5: (a) & (b) respectively show the configuration P and Q of sample mounting in the cryostat. The sample stage has a non-zero tilt(δ) with respect to the x - y plane.(c)AMR of the trilayer measured at 15K in configuration P and Q, and at 40K in configuration P.